INSTITUTE OF PHYSICS PUBLISHING JOURNAL OF MICROMECHANICS AND MICROENGINEERING

J. Micromech. Microeng. **14** (2004) 1119–1125 PII: S0960-1317(04)72209-3

Pull-in instability study of carbon nanotube tweezers under the influence of van der Waals forces

Gen-Wei Wang[1,2], Yin Zhang[1], Ya-Pu Zhao[1] and Gui-Tong Yang[2]

[1] State Key Laboratory of Nonlinear Mechanics (LNM), Institute of Mechanics, Chinese Academy of Sciences, Beijing 100080, People's Republic of China
[2] Institute of Applied Mechanics, Taiyuan University of Technology, Taiyuan 030024, Shanxi, People's Republic of China

E-mail: yzhao@lnm.imech.ac.cn

Received 17 November 2003
Published 17 June 2004
Online at stacks.iop.org/JMM/14/1119
doi:10.1088/0960-1317/14/8/001

Abstract
The pull-in instability of two nanotubes under van der Waals force is studied. The cantilever beam with large deformation model is used. The influence of nanotube parameters such as the interior radius, the gap distance between the two nanotubes, etc, on the pull-in instability is studied. The critical nanotube length is determined for each specific set of nanotube parameters. The Galerkin method is applied to discretize the governing equations, and it shows good convergence.

Nomenclature

A	Hamaker constant, $A = \pi^2 C \rho_1 \rho_2$
A_1, A_2	nanotube cross-section areas, $A_1 = \pi\left(r_2^2 - r_1^2\right)$ and $A_2 = \pi\left(r_4^2 - r_3^2\right)$
C	coefficient in the atom–atom pair potential
D	distance between the two nanotubes' edges
E	nanotube Young's modulus
I_1, I_2	moments of inertia of the nanotubes, $I_1 = \pi\left(r_2^4 - r_1^4\right)/4$ and $I_2 = \pi\left(r_4^4 - r_3^4\right)/4$
r_1, r_3	nanotube interior radii
r_2, r_4	nanotube exterior radii
L	nanotube length
N_1, N_2	axial forces on the two nanotubes
T	distance between the two nanotubes neutral axes, $T = D + r_2 + r_4$
t	nanotube thickness
u_1, u_2	nanotube deflections
U_1, U_2	nanotube dimensionless deflections
ρ_1, ρ_2	number of atoms per unit volume in the two bodies

Dimensionless ratios:

$R_2 = r_2/r_1$, $R_3 = r_3/r_1$, $R_4 = r_4/r_1$, $\beta = \frac{r_1}{T}$, $\eta = \frac{AL^4}{2\sqrt{2}E(r_1 T)^{7/2}}$

1. Introduction

The rapid growth of micro/nanoscale fabrication technologies in recent years has led to the development of various micro/nanoelectromechanical systems (MEMS/NEMS). Cantilever-based MEMS/NEMS structures such as microcantilever sensors [1, 2], microaccelerometers [3], atomic force microscopes (AFM) [4–6], microswitches [7, 8] etc are widely used. Since their discovery, carbon nanotubes have generated various application ideas due to their remarkable properties. Nanotweezers are one of the carbon nanotube applications. Kim and Lieber [9] were the first to attach two carbon nanotube bundles to a tapered glass structure to fabricate nanoscale tweezers. Voltage is applied to the electrode to open and close the free ends of the cantilever nanotubes. Akita *et al* [10] attached two carbon nanotubes to the metal electrodes patterned on a conventional Si tip to fabricate such nanotweezers. As the structure scale reaches the micro/nano level, the forces such as Casimir [11] and van der Waals (vdW) [12, 13] have a lot of influence on the structures. Dequesnes *et al* [13] studied the cantilever nanotube pull-in instability under the influence of vdW and electrical forces. Their vdW force is the nanotube–substrate force, which is not applied to nanotweezers' nanotube–nanotube structure. During their derivation of vdW force, the single-wall carbon nanotube

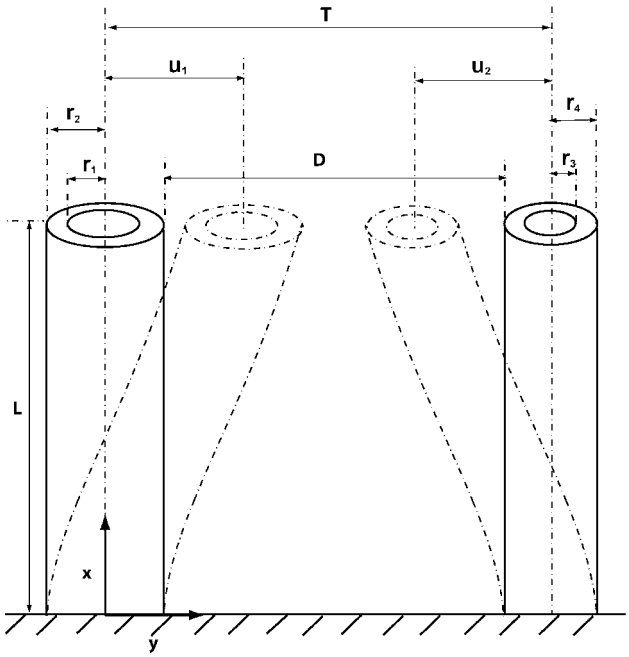

Figure 1. Schematic diagram of the two nanotubes and the coordinate system.

structure is modelled as a solid structure, which may not be applicable to the nanotube structure with relatively large interior radius. This paper presents a more general model, which calculates the vdW force by considering the influence of the nanotube interior and exterior radii and modelling the nanotube as a continuous system. Rotkin [14] obtains the analytical solution of the nanotube–substrate system by modelling the system as a one degree of freedom system and setting the first and second derivatives of the system's total energy to be zero. As the nanotube–substrate structure also forms a capacitance-like structure, the electrical force together with vdW force is included in Rotkin's model.

The model presented in this paper is the pull-in instability study of the nanotube–nanotube structure, which is a more suitable model for nanotweezers' structure. Dequesnes's pull-in criterion is based on the study of a system with one degree of freedom, which is not true for a continuous system. In this paper, the pull-in instability is found by studying the structure deflection curve slope. In this paper, vdW force is the sole force causing pull-in instability. For nanotweezers without an electrical actuation, vdW force is the dominant force. The critical design data can be obtained for nanotweezers by studying the pull-in instability under vdW force. The nanotube is modelled as a cantilever beam structure. The influence of the gap distance between the two nanotubes and the different interior and exterior radii on the pull-in instability is studied. The pull-in instability of several nanotube structures is compared.

2. Model development

2.1. Equilibrium equation

Consider the two cantilevered carbon nanotubes under vdW force in figure 1. The total vdW energy is computed by the double volume integral of the Lennard–Jones potential [13, 15, 16],

$$E_{\mathrm{vdW}}(r) = \int_{V_1}\int_{V_2} \frac{C\rho_1\rho_2}{r^6}\,\mathrm{d}V_1\,\mathrm{d}V_2,$$

where V_1 and V_2 are the two (volume) domains of the integration, ρ_1, ρ_2 are the number of atoms per unit volume in the two bodies and r is the distance between any points in bodies V_1 and V_2. For the two-nanotube shell-like structure, E_{vdW} is obtained by superposing the four-solid-cylinder vdW energy [17] as

$$E_{\mathrm{vdW}}(shell1, shell2) = E_{\mathrm{vdW}}(sc2, sc4) - E_{\mathrm{vdW}}(sc2, sc3) - E_{\mathrm{vdW}}(sc1, sc4) + E_{\mathrm{vdW}}(sc1, sc3).$$

Here *shell*1 is the (hollow) cylinder with interior radius r_1 and exterior radius r_2, *shell*2 is the (hollow) cylinder with interior radius r_3 and exterior radius r_4. $sc1$ is the solid cylinder with radius r_1, $sc2$ is the solid cylinder with radius r_2, $sc3$ is the solid cylinder with radius r_3 and $sc4$ is the solid cylinder with radius r_4. Thus, the two nanotubes' vdW energy E_{vdW} is computed by using the formula given by Israelachvili [16] for the solid cylinder as

$$E_{\mathrm{vdW}} = -\frac{AL}{12\sqrt{2}}\left[\frac{1}{(D-u_1-u_2)^{3/2}}\left(\frac{r_2r_4}{r_2+r_4}\right)^{1/2} - \frac{1}{(D+t-u_1-u_2)^{3/2}}\left(\frac{r_2r_3}{r_2+r_3}\right)^{1/2} - \frac{1}{(D+t-u_1-u_2)^{3/2}}\left(\frac{r_1r_4}{r_1+r_4}\right)^{1/2} + \frac{1}{(D+2t-u_1-u_2)^{3/2}}\left(\frac{r_1r_3}{r_1+r_3}\right)^{1/2}\right],$$

where A is the Hamaker constant, L is the nanotube cylinder length, D is the distance between the two nanotubes' edges. Here the two nanotubes are assumed to have the same thickness and length. u_1, u_2 are the two nanotubes' deflections and it is worth pointing out that u_1 is the coordinate of the first nanotube and u_2 is not the coordinate of the second nanotube as the coordinate system in the schematics of figure 1 shows. The coordinate of the second nanotube is $T-u_2$ and u_2 is a positive number. The vdW force f_{vdW} (per unit length) between the two nanotubes can be derived by taking the derivative $\mathrm{d}(E_{\mathrm{vdW}}/L)/\mathrm{d}D$ [13, 16]

$$f_{\mathrm{vdW}} = \frac{\mathrm{d}(E_{\mathrm{vdW}}/L)}{\mathrm{d}D} = \frac{A}{8\sqrt{2}}\left[\frac{1}{(D-u_1-u_2)^{5/2}}\left(\frac{r_2r_4}{r_2+r_4}\right)^{1/2} - \frac{1}{(D+t-u_1-u_2)^{5/2}}\left(\frac{r_2r_3}{r_2+r_3}\right)^{1/2} - \frac{1}{(D+t-u_1-u_2)^{5/2}}\left(\frac{r_1r_4}{r_1+r_4}\right)^{1/2} + \frac{1}{(D+2t-u_1-u_2)^{5/2}}\left(\frac{r_1r_3}{r_1+r_3}\right)^{1/2}\right].$$

The vdW force $f_{\mathrm{vdW}}(u_1, u_2)$ is a coupled nonlinear equation.

Here the governing equation is developed individually for each nanotube for reasons of brevity. The equilibrium equations derived by this method are no different from the

equations derived by writing the system energy together. For nanotube 1, the elastic bending energy U_{B1} is

$$U_{B1} = \frac{EI_1}{2}\int_0^L \left(\frac{\partial^2 u_1}{\partial x^2}\right)^2 \mathrm{d}x,$$

where EI_1 is the bending stiffness for nanotube 1. And the elastic stretching energy U_{s1} due to the axial force N_1 is

$$U_{s1} = \frac{N_1}{2}\int_0^L \left(\frac{\partial^2 u_1}{\partial x^2}\right)^2 \mathrm{d}x.$$

For the case of the nanotube studied here, there is no axial force, i.e. $N_1 = 0$, $U_{s1} = 0$. The nanotube elastic stretching energy U_{N1} due to the large deformation is [18]

$$U_{N1} = \frac{A_1 E}{2L}\left[\frac{1}{2}\int_0^L \left(\frac{\partial u_1}{\partial x}\right)^2 \mathrm{d}x\right]^2,$$

where A_1 is the cross-section area of nanotube 1, E is the nanotube Young's modulus. The work W_{vdW1} done by the vdW force f_{vdW} is

$$W_{\mathrm{vdW1}} = \int_0^L \int_0^{u_1} f_{\mathrm{vdW}}\,\mathrm{d}u\,\mathrm{d}x.$$

By using the principle of virtual work (PVW) $\delta(U_{B1} + U_{s1} + U_{N1} - W_{\mathrm{vdW1}}) = 0$, the governing equation is derived as

$$EI_1\frac{\partial^4 u_1}{\partial x^4} = \frac{EA_1}{2L}\frac{\partial^2 u_1}{\partial x^2}\int_0^L \left(\frac{\partial u_1}{\partial x}\right)^2 \mathrm{d}x + f_{\mathrm{vdW}}(u_1, u_2). \quad (1)$$

Similarly, the equilibrium equation for the second nanotube is derived as

$$EI_2\frac{\partial^4 u_2}{\partial x^4} = \frac{EA_2}{2L}\frac{\partial^2 u_2}{\partial x^2}\int_0^L \left(\frac{\partial u_2}{\partial x}\right)^2 \mathrm{d}x + f_{\mathrm{vdW}}(u_1, u_2). \quad (2)$$

Once again, it is pointed out that u_2 is not the coordinate of the second nanotube. Equations (1) and (2) do obey Newton's third law that the vdW force f_{vdW} acting on nanotube 1 has the same magnitude as the vdW force acting on nanotube 2 but the opposite direction. For the cantilever beam structure, the boundary conditions are

$$\begin{aligned} &u_1(0) = 0, && \frac{\partial u_1(0)}{\partial x} = 0,\\ &\frac{\partial^2 u_1(L)}{\partial x^2} = 0, && \frac{\partial^3 u_1(L)}{\partial x^3} = 0, \end{aligned} \quad (3)$$

and

$$\begin{aligned} &u_2(0) = 0, && \frac{\partial u_2(0)}{\partial x} = 0,\\ &\frac{\partial^2 u_2(L)}{\partial x^2} = 0, && \frac{\partial^3 u_2(L)}{\partial x^3} = 0. \end{aligned} \quad (4)$$

2.2. Nondimensionalization

To nondimensionalize equations (1) and (2), the following dimensionless numbers are introduced

$$\xi = \frac{x}{L}, \qquad U_1 = \frac{u_1}{T}, \qquad U_2 = \frac{u_2}{T}, \qquad \beta = \frac{r_1}{T}.$$

Equations (1) and (2) are nondimensionalized as

$$U_1^{(4)} = \frac{2}{(R_2^2+1)\beta^2}U_1''\int_0^1 (U_1)'^2\,\mathrm{d}\xi + \frac{\eta}{R_2^4 - 1}F_{\mathrm{vdW}}(U_1, U_2). \quad (5)$$

Here $(\,)' = \frac{\partial}{\partial\xi}$, $(\,)^{(4)} = \frac{\partial^4}{\partial\xi^4}$ and $F_{\mathrm{vdW}}(U_1, U_2)$ is defined as

$$\begin{aligned} F_{\mathrm{vdW}} = {} & \frac{1}{(1-\beta R_2 - \beta R_4 - U_1 - U_2)^{5/2}}\left(\frac{R_2R_4}{R_2+R_4}\right)^{1/2}\\ & - \frac{1}{(1-\beta R_2 - \beta R_3 - U_1 - U_2)^{5/2}}\left(\frac{R_2R_3}{R_2+R_3}\right)^{1/2}\\ & - \frac{1}{(1-\beta - \beta R_4 - U_1 - U_2)^{5/2}}\left(\frac{R_4}{1+R_4}\right)^{1/2}\\ & + \frac{1}{(1-\beta - \beta R_3 - U_1 - U_2)^{5/2}}\left(\frac{R_3}{1+R_3}\right)^{1/2}, \end{aligned}$$

and

$$U_2^{(4)} = \frac{2}{(R_3^2+R_4^2)\beta^2}U_2''\int_0^1 (U_2)'^2\,\mathrm{d}\xi + \frac{\eta}{R_4^4 - R_3^4}F_{\mathrm{vdW}}(U_1, U_2), \quad (6)$$

where $\frac{2}{(R_2^2+1)\beta^2}$ and $\frac{2}{(R_3^2+R_4^2)\beta^2}$ are the parameters indicating the nonlinear stretching part contribution to the total nanotube bending deflection. β is the parameter indicating the relationship between the nanotube size and distance between the two nanotubes (the nanotube thickness here is assumed to be fixed). In all the examples computed in this paper, β is a very small number. So the nonlinear part contribution to the governing equation may be relatively important. Its contribution also depends on U_i'' and $(U_i')^2$ $(i = 1, 2)$, which are unknown. The vdW energy has the order of [16] $E_{\mathrm{vdW}} \propto \frac{AL}{D^{3/2}}r_1^{1/2}$, and the nanotube bending energy has the order of $E_{\mathrm{bending}} \propto EI\int_0^L \left(\frac{\mathrm{d}^2u}{\mathrm{d}x^2}\right)^2 \mathrm{d}z \propto Er_1^4\left(\frac{D}{L^2}\right)^2 L = Er_1^4\frac{D^2}{L^3}$, so the ratio is as follows:

$$\frac{E_{\mathrm{vdW}}}{E_{\mathrm{bending}}} \propto \frac{AL}{D^{3/2}}r_1^{1/2}\frac{L^3}{Er_1^4D^2} = \frac{AL^4}{E(r_1D)^{7/2}} \propto \eta.$$

Here η only indicates the order of the ratio of the two energies, not the actual ratio because the critical parameter, the thickness is not shown in η.

The boundary conditions are also nondimensionalized as

$$\begin{aligned} &U_1(0) = 0, && U_1'(0) = 0,\\ &U_1''(1) = 0, && U_1'''(1) = 0, \end{aligned} \quad (7)$$

and

$$\begin{aligned} &U_2(0) = 0, && U_2'(0) = 0,\\ &U_2''(1) = 0, && U_2'''(1) = 0. \end{aligned} \quad (8)$$

2.3. Galerkin method

In order to compute the coupled nonlinear equations (5) and (6), the Galerkin method is applied to discretize the two equilibrium equations. U_1 and U_2 are assumed to have the following expansions,

$$U_1(\xi) = \sum_{i=1}^{N} a_i\phi_i(\xi), \quad (9)$$

and

$$U_2(\xi) = \sum_{i=1}^{N} b_i\phi_i(\xi), \quad (10)$$

where N is the mode number and a_i, b_i are the unknown constants to be determined. $\phi_i(\xi)$ is the cantilever beam

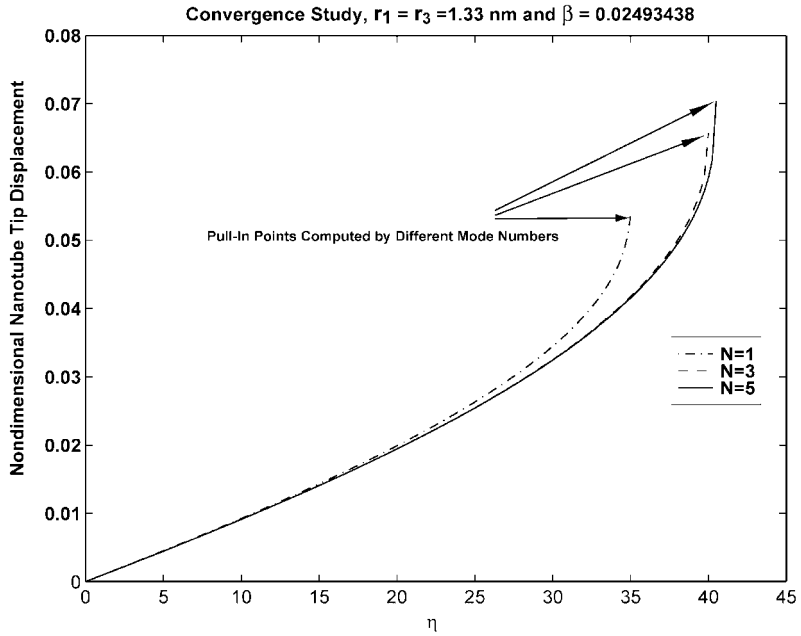

Figure 2. Convergence study as the mode number changes. $r_1 = r_3 = 1.33$ nm, $t = 0.34$ nm and $D = 50$ nm.

mode shape given by Craig and Chang [19]. The asymptotic approximation and simpler expression of $\phi_i(\xi)$ are given by Dowell [20] and Dugundji [21]. In this paper, Craig and Chang's mode shape is used. By substituting U_1, U_2 in equations (9) and (10) into equations (5) and (6), multiplying equations (5), (6) by $\phi_i(\xi)$ and then integrating from 0 to 1, the equilibrium equations are changed as

$$\begin{cases} \int_0^1 \phi_1 \left\{ \sum_{i=1}^N a_i \phi_i^{(4)} - \left[\frac{2}{(R_2^2+1)\beta^2} \int_0^1 \left(\sum_{i=1}^N b_i \phi_i' \right)^2 \mathrm{d}\xi \sum_{i=1}^N a_i \phi_i'' + \frac{\eta}{R_2^4-1} F_{\mathrm{vdW}} \right] \right\} \mathrm{d}\xi = 0 \\ \int_0^1 \phi_2 \left\{ \sum_{i=1}^N a_i \phi_i^{(4)} - \left[\frac{2}{(R_2^2+1)\beta^2} \int_0^1 \left(\sum_{i=1}^N b_i \phi_i' \right)^2 \mathrm{d}\xi \sum_{i=1}^N a_i \phi_i'' + \frac{\eta}{R_2^4-1} F_{\mathrm{vdW}} \right] \right\} \mathrm{d}\xi = 0 \\ \cdots\cdots\cdots\cdots\cdots\cdots\cdots\cdots\cdots\cdots\cdots\cdots\cdots\cdots\cdots\cdots\cdots\cdots\cdots\cdots\cdots\cdots\cdots\cdots\cdots\cdots\cdots\cdots\cdots\cdots \\ \int_0^1 \phi_N \left\{ \sum_{i=1}^N a_i \phi_i^{(4)} - \left[\frac{2}{(R_2^2+1)\beta^2} \int_0^1 \left(\sum_{i=1}^N b_i \phi_i' \right)^2 \mathrm{d}\xi \sum_{i=1}^N a_i \phi_i'' + \frac{\eta}{R_2^4-1} F_{\mathrm{vdW}} \right] \right\} \mathrm{d}\xi = 0 \\ \int_0^1 \phi_1 \left\{ \sum_{i=1}^N b_i \phi_i^{(4)} - \left[\frac{2}{(R_3^2+R_4^2)\beta^2} \int_0^1 \left(\sum_{i=1}^N b_i \phi_i' \right)^2 \mathrm{d}\xi \sum_{i=1}^N b_i \phi_i'' + \frac{\eta}{R_4^4-R_3^4} F_{\mathrm{vdW}} \right] \right\} \mathrm{d}\xi = 0 \\ \int_0^1 \phi_2 \left\{ \sum_{i=1}^N b_i \phi_i^{(4)} - \left[\frac{2}{(R_3^2+R_4^2)\beta^2} \int_0^1 \left(\sum_{i=1}^N b_i \phi_i' \right)^2 \mathrm{d}\xi \sum_{i=1}^N b_i \phi_i'' + \frac{\eta}{R_4^4-R_3^4} F_{\mathrm{vdW}} \right] \right\} \mathrm{d}\xi = 0 \\ \cdots\cdots\cdots\cdots\cdots\cdots\cdots\cdots\cdots\cdots\cdots\cdots\cdots\cdots\cdots\cdots\cdots\cdots\cdots\cdots\cdots\cdots\cdots\cdots\cdots\cdots\cdots\cdots\cdots\cdots \\ \int_0^1 \phi_N \left\{ \sum_{i=1}^N b_i \phi_i^{(4)} - \left[\frac{2}{(R_3^2+R_4^2)\beta^2} \int_0^1 \left(\sum_{i=1}^N b_i \phi_i' \right)^2 \mathrm{d}\xi \sum_{i=1}^N b_i \phi_i'' + \frac{\eta}{R_4^4-R_3^4} F_{\mathrm{vdW}} \right] \right\} \mathrm{d}\xi = 0. \end{cases} \tag{11}$$

There are $2 \times N$ equations and $2 \times N$ unknowns (a_i, b_i, $i =$ 1 to N). The Newton–Rhapson method is applied to solve the nonlinear equations.

3. Results and discussion

Figure 2 shows the convergence study of different mode numbers on the computation. D is taken as 50 nm, $r_1 = r_3 = 1.33$ nm, $E = 1$ TPa and $t = 0.34$ nm. As the mode number is chosen as 1, 3 and 5, the pull-in η is 35, 40 and 40.5 respectively. The pull-in η value converges at 40.5 with further mode number increasing. The physical meaning of parameter η is mentioned above as the order of the two energies' (vdW and bending energies) ratio. From the definition of η $\left(\eta = \frac{AL^4}{2\sqrt{2}E(r_1 T)^{7/2}}\right)$ in the nomenclature, η can be changed by changing the Hamaker constant (A), or nanotube length (L), or Young's modulus (E) or nanotube interior radius (r_1), or the distance between the two nanotubes' neutral axes (T). If the material properties of the nanotubes (A, L, E, r_1) are fixed, the only and direct way of changing η is to change the distance between the two nanotubes' neutral axes (T) and $\eta \propto 1/T^{7/2}$. We also change η by changing T, r_1 and L together (see figures 6 and 7) to achieve pull-in values. Because in figure 2 the two nanotubes have the same interior radii, thickness, length and Young's modulus, U_1 has the same value as U_2. Clearly the pull-in nanotube tip deflections $U_1(1)$ and $U_2(1)$ do not converge well as the mode number increases. Increasing mode number does not improve the convergence of U_1 and U_2. As the system approaches the pull-in point, the

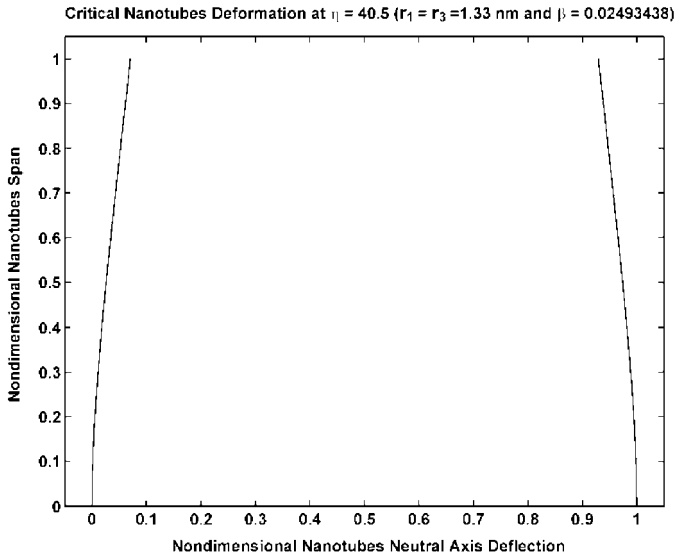

Figure 3. The two nanotubes' neutral axes deflection at the pull-in. $\eta = 40.5$, $r_1 = r_3 = 1.33$ nm, $t = 0.34$ nm.

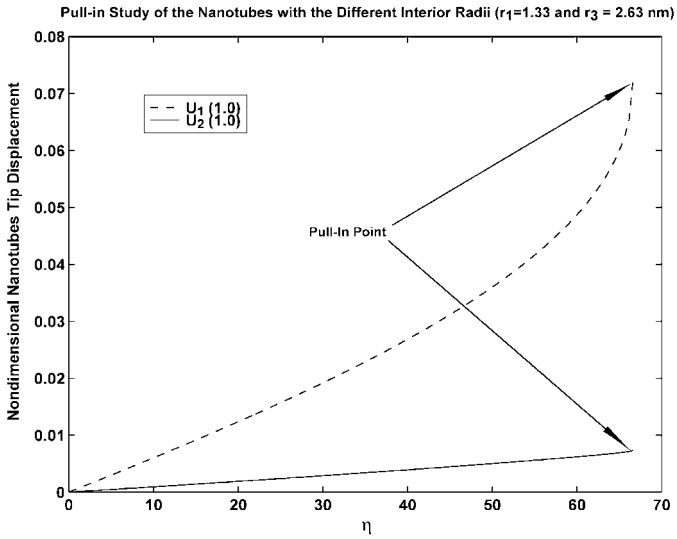

Figure 4. Pull-in study of two nanotubes with different interior radii. $r_1 = 1.33$ nm, $r_3 = 2.63$ nm, $t = 0.34$ nm and $D = 50$ nm.

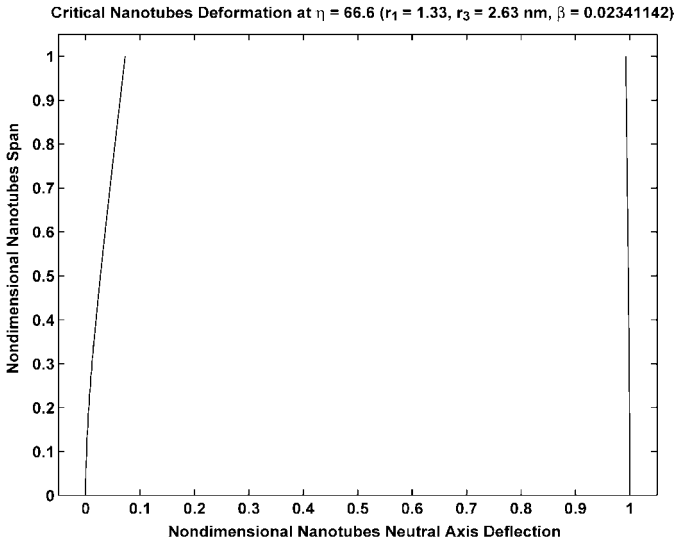

Figure 5. The two neutral axes pull-in deflection of the nanotubes with different interior radii at $\eta = 66.6$. $r_1 = 1.33$ nm, $r_3 = 2.63$ nm, $t = 0.34$ nm and $D = 50$ nm.

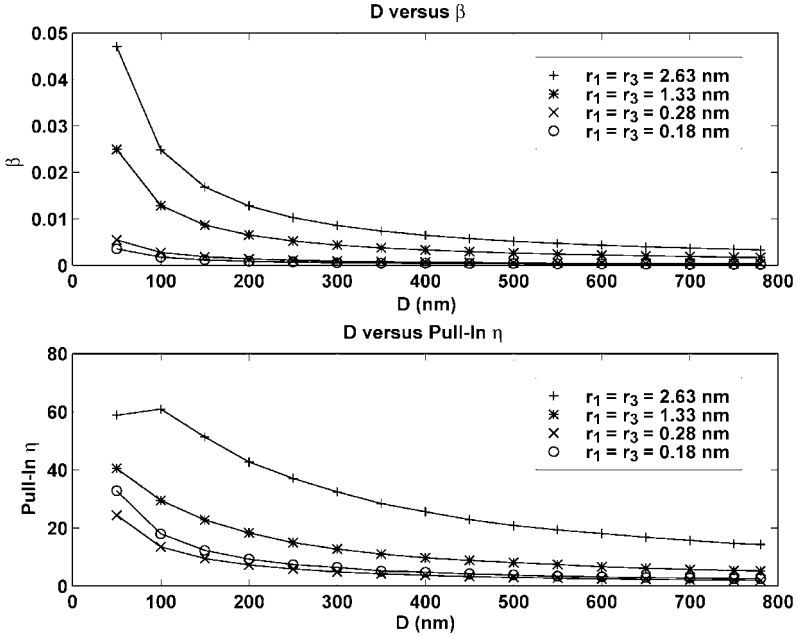

Figure 6. β and pull-in η for the two nanotube system with the same interior radii, with changing D.

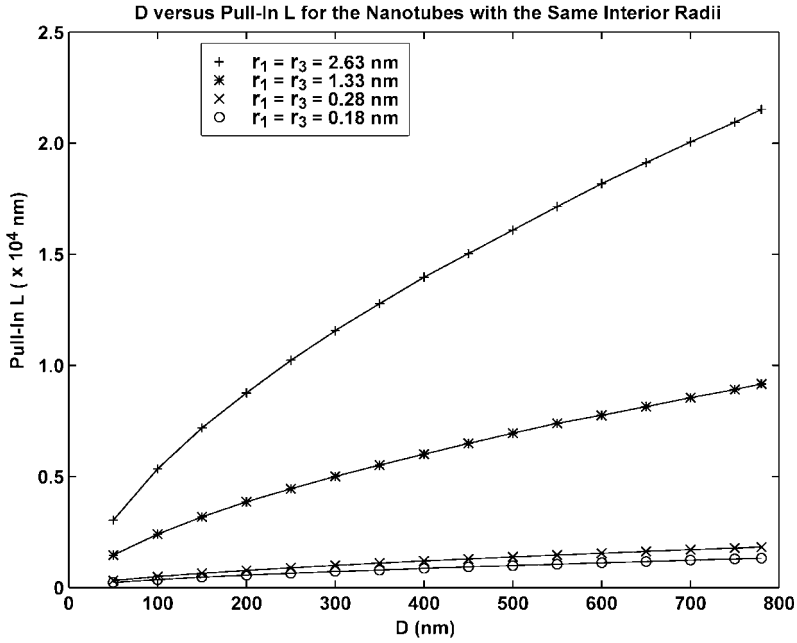

Figure 7. Pull-in nanotube length L for the two nanotube system with the same interior radii, with changing D.

curve slope increases dramatically. When the slope is infinite, pull-in happens [22]. There is also the numerical difficulty of finding the pull-in displacement. Any small η change around the pull-in point will cause large U_i $(i = 1, 2)$ change. The critical pull-in U_i $(i = 1, 2)$ largely depends on the step size of η. In this paper, all the computation results are obtained by using five mode shapes. Because most researchers adopt $E =$ 1 TPa and $t = 0.34$ nm for single-wall carbon nanotubes [23], this paper assumes such Young's modulus and thickness unless other Young's modulus and thickness are specified. Figure 3 shows the two nanotubes' neutral axes deflection at the critical pull-in point $\eta = 40.5$ obtained from figure 2. Figure 4 shows the two nanotubes with different radii, $r_1 = 1.33$ nm and $r_3 = 2.63$ nm. For the nanotube with larger interior radius (the two nanotubes have the same thickness), its larger bending stiffness (EI) will cause smaller deflection because the vdW force acting on the two nanotubes has the same magnitude but the opposite direction. Figure 5 shows the deflection of the two nanotubes' neutral axes at the pull-in $\eta = 66.6$.

Figure 6 shows β and pull-in η of the nanotubes with the same interior radii as D changes. The interior radii r_1 and r_3 are chosen as 2.63 nm, 1.33 nm [24], 0.28 nm [25] and 0.18 nm [26]. D starts from 50 nm to 780 nm. From figure 6, β decreases monotonically but pull-in η does not as D increases. Figure 7 shows the pull-in nanotube length L, which is computed from pull-in η, as D changes. Here the

Hamaker constant A is taken as 23.8×10^{-20} J [27]. Clearly in figure 7, the pull-in length L increases monotonically as D increases. As D increases, the vdW force reduces and for each individual set of nanotubes, the thickness and interior radii do not change, thus, the nanotube cross-section bending stiffness (EI) does not change, either. In such a case, increasing the nanotube length, which reduces the system flexibility, is the only way to let the carbon nanotube system reach the pull-in instability.

4. Conclusion

The pull-in instability of a tweezer-like nanostructure is studied. The pull-in points of the two-nanotube system are found by studying the nanotube neutral axes deflection curve as its slope approaches infinity. The influence of the two nanotubes' distance and interior radii on the pull-in instability is analysed. For the nanotubes with the different interior radii, the pull-in nanotube length is given. This pull-in instability study offers data on the nanotube gap size and length for nanotweezers design. The model accounts for the large deformation as a nonlinear part in the governing equations, which can be easily extended to the study of other structures under the vdW force influence. However, during the derivation of vdW force, the model does not account for the nanotube interlayer interaction. Thus the model may not be applied to the analysis of a multi-wall nanotube structure under vdW force.

Acknowledgments

This research was supported by the National Natural Science Foundation of China (NSFC) (grant no 10225209 and no 90305020), key project from the Chinese Academy of Sciences (grant no KJCX2-SW-L2), NSFC-RGC Joint Project (grant no 50131160739) and the '973' project (grant no 1999033103).

References

[1] Thundat T, Oden P I and Warmack R J 1997 Microcantilever sensors *Thermophys. Eng.* **1** 185–99

[2] Du L, Kwon G, Arai F, Fukuda T, Itoigawa K and Tukahara Y 2003 Structure design of micro touch sensor array *Sensors Actuators* A **107** 7–13

[3] Kovács A and Vízváry Z 2001 Structural parameter sensitivity analysis of cantilever- and bridge-type accelerometers *Sensors Actuators* A **89** 197–205

[4] Raiteri R and Butt H J 1995 Measuring electrochemically induced surface stress with an atomic force microscope *J. Phys. Chem.* **99** 15728–32

[5] Miyahara Y, Deschler M, Fujii T, Watanabe S and Bleuler H 2002 Non-contact atomic force microscope with a PZT cantilever used for deflection sensing, direct oscillation and feedback actuation *Appl. Surf. Sci.* **188** 450–5

[6] Ishikawa M, Yoshimura M and Ueda K 2002 Carbon nanotube as a probe for friction force microscopy *Physica* B **323** 184–6

[7] Adamschik M, Kusterer J, Schmid P, Schad K B, Grobe D, Flöter A and Kohn E 2002 Diamond microwave relay *Diam. Rel. Mater.* **11** 672–6

[8] Ruan M, Shen J and Wheeler C B 2001 Latching microelectromagnetic relays *Sensors Actuators* A **91** 346–50

[9] Kim P and Lieber C M 1999 Nanotube nanotweezers *Science* **286** 2148–50

[10] Akita S, Nakayama Y, Mizooka S, Takano Y, Okawa T, Miyatake Y, Yamanaka S, Tsuji M and Nosaka T 2001 Nanotweezers consisting of carbon nanotubes operating in an atomic force microscope *Appl. Phys. Lett.* **79** 1691–3

[11] Buks E and Roukes M 2001 Stiction, adhesion energy and the Casimir effect in micromechanical systems *Phys. Rev.* B **63** 033402

[12] Lin W H and Zhao Y P 2003 Dynamics behavior of nanoscale electrostatic actuators *Chin. Phys. Lett.* **20** 2070–3

[13] Dequesnes M, Rotkin S V and Aluru N R 2002 Calculation of pull-in voltages for carbon-nanotube-based nanoelectromechanical switches *Nanotechnology* **13** 120–31

[14] Rotkin S V 2003 Theory of Nanotube Nanodevices *Nanostructured Materials and Coatings for Biomedical and Sensor Applications* ed Y G Gogotsi and I V Uvarova (Dordrecht: Kluwer) pp 257–77

[15] Girifalco L A 1992 Molecular properties of C_{60} in the gas and solid phases *J. Phys. Chem.* **96** 858–61

[16] Israelachvili J N 1985 *Intermolecular and Surface Forces with Applications to Colloidal and Biological Systems* (New York: Academic) p 138

[17] Tadmor R 2001 The London–van der Waals interaction energy between objects of various geometries *J. Phys.: Condens. Matter* **13** L195–L202

[18] McDonald P H Jr 1955 Nonlinear dynamic coupling in a beam vibration *J. Appl. Mech.* **22** 573–8

[19] Chang T C and Craig R R Jr 1969 Normal modes of uniform beams *J. Eng. Mech. Div. ASCE* **195** 1027–31

[20] Dowell E H 1984 On asymptotic approximations to beam model shapes *J. Appl. Mech.* **51** 439

[21] Dugundji J 1988 Simple expression for higher vibration modes of uniform Euler beams *AIAA J.* **26 8** 1013–4

[22] Zhang X M, Chau F S, Quan C, Lam Y L and Liu A Q 2001 A study of the static characteristics of a torsional micromirror *Sensors Actuators* A **90** 73–81

[23] Ru C Q 2004 Elastic models for carbon nanotubes *Encyclopedia of Nanoscience and Nanotechnology* ed H S Nalwa (Stevenson Ranch, CA: American Scientific Publishers) (at press)

[24] Lebedkin S, Schweiss P, Renker B, Malik S, Hennrich F, Neumaier M, Stoermer C and Kappes M M 2002 Single-wall carbon nanotubes with diameters approaching 6 nm obtained by laser vaporization *Carbon* **40** 417–23

[25] Strong K L, Anderson D P, Lafdi K and Kuhn J N 2003 Purification process for single-wall carbon nanotubes *Carbon* **41** 1477–88

[26] Ajayan P M and Iijima S 1992 Smallest carbon nanotube *Nature* **358** 23

[27] Peukert W, Mehler C and Götzinger M 2002 Novel concepts for characterisation of heterogeneous particulate surfaces *Appl. Surf. Sci.* **196** 30–40